Multinuclear NMR, X-ray, and DFT Studies on RhCl(diene)(phosphoramidite) Complexes

Serena Filipuzzi, Elisabeth Männel, and Paul S. Pregosin*

Laboratory of Inorganic Chemistry, ETH, Zürich, CH-8093, Switzerland

Alberto Albinati* and Silvia Rizzato

Department of Structural Chemistry (DCSSI), University of Milan, 20133 Milan, Italy
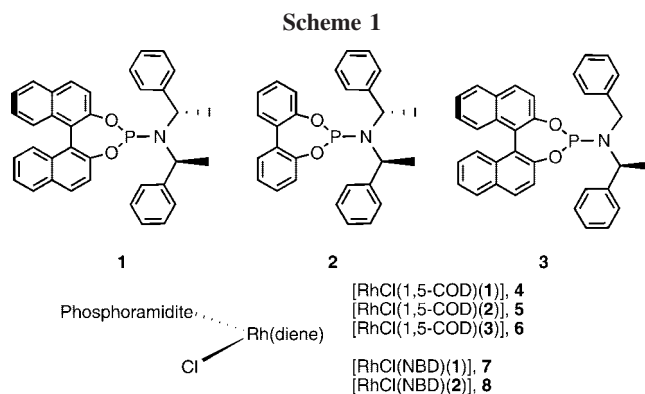
Luis F. Veiros*

Centro de Química Estrutural, Complexo I, Instituto Superior Técnico, Avenida Rovisco Pais 1, 1049-001 Lisbon, Portugal

NMR, X-ray, and DFT studies on several [RhCl(diene)(phosphoramidite)] complexes suggest that both electronic and steric effects affect the nature of the olefin, chloride, and P-donor bonding. The X-ray study of [RhCl(1,5-COD)(phosphoramidite)] (phosphoramidite = (Binol)PN(CH(CH$_3$)Ph)$_2$) reveals an intramolecular selectivity in the back-bonding in which the C−C bond of the olefin *trans* to the Cl ligand is preferentially elongated. Two types of dynamic processes have been detected at ambient temperature in CD$_2$Cl$_2$ solution using 2-D NOESY methods: presumed phosphoramidite dissociation and diolefin rotation. The former is observed with both 1,5-COD and NBD. The latter is more selective in that the intramolecular dynamics for the NBD analogues are relatively fast, but those for the 1,5-COD compounds, barely detectable. DFT calculations suggest that the diolefin rotation proceeds over a tetrahedral transition state and that there is a smaller energy barrier for the NBD complexes relative to the analogous 1,5-COD species. Two bis phosphoramidite salts of the form [Rh(1,5-COD)(phosphoramidite)$_2$]BF$_4$ are reported.

Introduction

Monodentate chiral phosphorus ligands are finding increasing use in homogeneous catalysis.[1,2] Phosphoramidites are among the most frequently used, as these have been shown[2] to be excellent auxiliaries in homogeneous hydrogenation, allylic alkylation, and other reactions. As these ligands are easily prepared,[2d,e,g] one finds a relatively large number of structural variations on these P-donors. There are a number of reports concerned with rhodium complexes of such ligands, primarily in connection with hydrogenation chemistry.[3] Occasionally, the steric bulk of the phosphoramidite is thought to be important,

Scheme 1

1　　　　　　2　　　　　　3

Phosphoramidite....Rh(diene) / Cl

[RhCl(1,5-COD)(**1**)], **4**
[RhCl(1,5-COD)(**2**)], **5**
[RhCl(1,5-COD)(**3**)], **6**

[RhCl(NBD)(**1**)], **7**
[RhCl(NBD)(**2**)], **8**

although there are few studies that clearly separate steric and electronic effects.[2h]

In this contribution we report on a selection of neutral [RhCl(1,5-COD)(phosphoramidite)] and [RhCl(NBD)(phosphoramidite)] derivatives, using ligands **1**−**3** (see Scheme 1) and discuss aspects of their bonding and dynamics via multinuclear NMR, X-ray, and DFT methods.

Results and Discussion

The chiral phosphoramidite complexes, **4**−**8**, were all prepared via the usual bridge splitting reactions starting from the chloro-bridged dinuclear rhodium olefin complexes and (with respect to the amino side chain) the enantiopure phosphoramidites.
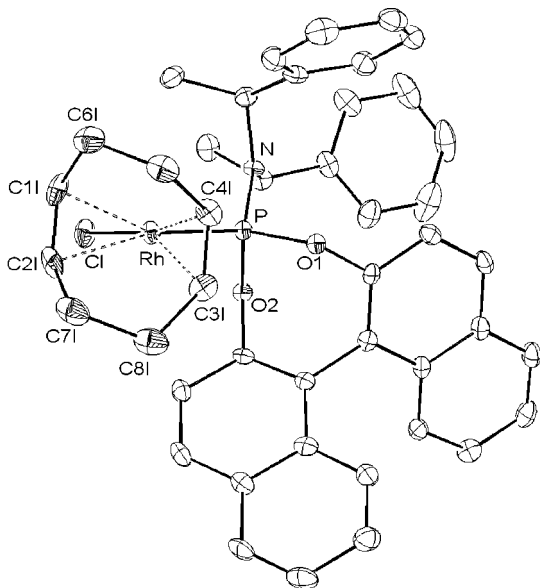
* Corresponding authors. E-mail: pregosin@inorg.chem.ethz.ch.

(1) (a) Hayashi, T. *Acc. Chem. Res.* **2000**, *33*, 354–362. (b) Hayashi, T. *J. Synth. Org. Chem. Jpn.* **1994**, *52*, 900–911. (c) Feringa, B. L. *Acc. Chem. Res.* **2000**, *33*, 346.

(2) (a) Imbos, R.; Minnaard, A. J.; Feringa, B. L. *Dalton Trans.* **2003**, 2017–2023. (b) Pena, D.; Minnaard, A. J.; de Vries, J. G.; Feringa, B. L. *J. Am. Chem. Soc.* **2002**, *124*, 14552–14553. (c) Bayer, A.; Thewalt, U.; Rieger, B. *Eur. J. Inorg. Chem.* **2002**, *19*, 9–203. (d) Polet, D.; Alexakis, A.; Tissot-Croset, K.; Corminboeuf, C.; Ditrich, K. *Chem.−Eur. J.* **2006**, *12*, 3596–3609. (e) Monti, C.; Gennari, C.; Piarulli, U. *Chem.−Eur. J.* **2007**, *13*, 1547–1558. (f) de Vries, J. G.; Lefort, L. *Chem.−Eur. J.* **2006**, *12*, 4722–4734. (g) Christoffers, J.; Koripelly, G.; Rosiak, A.; Rossle, M. *Synthesis* **2007**, 1279–1300. (h) Flanagan, S. P.; Guiry, P. J. *J. Organomet. Chem.* **2006**, *691*, 2125–2154.

(3) (a) Reetz, M. T.; Ma, J. A.; Goddard, R. *Angew. Chem., Int. Ed.* **2005**, *44*, 412–415. (b) Reetz, M. T.; Bondarev, O. *Angew. Chem., Int. Ed.* **2007**, *46*, 4523–4526. (c) Reetz, M. T.; Mehler, G.; Bondarev, O. *Chem. Commun.* **2006**, 2292–2294. (d) Eberhardt, L.; Armspach, D.; Matt, D.; Toupet, L.; Oswald, B. *Eur. J. Inorg. Chem.* **2007**, *415*, 3–4161. (e) Minnaard, A. J.; Feringa, B. L.; Lefort, L.; De Vries, J. G. *Acc. Chem. Res.* **2007**, *40*, 1267–1277.

Figure 1. ORTEP view of the structure of **4**. Selected metric data: Rh−C(1L) 2.244(4); Rh−C(2L) 2.278(4); Rh−C(3L) 2.111(4); Rh−C(4L) 2.133(4); Rh−Cl 2.383(1); Rh−P 2.230(1); P−O(1) 1.636(3); P−O(2) 1.629(3); P−N 1.650(3); C(1L)−C(2L) 1.353(6); C(3L)−C(4L) 1.404(6); P−Rh−Cl 87.18(4); P−Rh−C(1L) 158.1(1); P−Rh−C(2L) 167.0(1); P−Rh−C(3L) 94.6(1); P−Rh−C(4L) 95.4(1); Cl−Rh−C(1L) 91.7(1); Cl−Rh−C(2L) 91.4(1); Cl−Rh−C(3L) 151.0(1); Cl−Rh−C(4L) 170.0(1); C(3L)−Rh−C(1L) 96.9(2); C(4L)−Rh−C(1L) 82.3(2); C(3L)−Rh−C(2L) 80.4(2); C(4L)−Rh−C(2L) 88.2(2); C(1L)−C(2L)−C(7L) 125.6(4); C(6L)−C(1L)−C(2L) 125.4(4); C(5L)−C(4L)−C(3L) 124.6(4); C(4L)−C(3L)−C(8L) 126.6(4).

Solid-State Structure of 4. Figure 1 shows a view of [RhCl(1,5-COD)(**1**)], **4**,[4] from behind the complexed 1,5-COD, and selected bond lengths and bond angles are given in the caption to the figure. The immediate coordination sphere consists of the phosphoramidite P-donor, the two complexed 1,5-COD double bonds, and the Rh−Cl interaction.
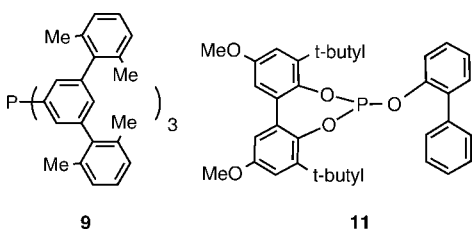
On the basis of a comparison of the various bond lengths from **4** with those from related Rh-1,5-COD complexes containing P(p-FC$_6$H$_4$)$_3$,[5a] PCl(SiMe$_3$)$_2$,[5b] the "bowl-shaped" phosphine **9** (in complex **10**[6]), and the bulky phosphite **11** (in complex **12**[7]), it would appear that, despite its relatively large size, phosphoramidite ligand **1** affords a shorter Rh−P bond and a slightly longer Rh−Cl bond (see Table 1) relative to the

Table 1. Selected Bond Lengths for the RhCl(1,5-COD)(phosphine) Complexes

complex	Rh−P	Rh−Cl	Rh−C1	Rh−C2	Rh−C3	Rh−C4
4	2.230(1)	2.383(1)	2.245(4)	2.279(4)	2.111(4)	2.133(4)
P(p-FC$_6$H$_4$)$_3$	2.130(8)	2.297(1)	2.366(2)	2.234(7)	2.216(6)	2.097(8)
PCl(SiMe$_3$)$_2$	2.287(1)	2.363(1)				
10[5]		2.285(1)	2.365(2)	2.208(7)	2.229(6)	2.115(7)	2.131(7)
12[7]		2.223(1)	2.358(1)	2.247(6)	2.291(5)	2.120(5)	2.144(5)

phosphine complexes. The slightly longer Rh−Cl bond might well arise from steric interactions involving the large organic substituents on the P atom. However, complex **12**, with the very bulky phosphite ligand **11** (see Table 1), shows bond lengths for all of the donors that are rather close to those for **4**.

The Rh−C(olefin) separations pseudo-*trans* to the phosphoramidite P-donor are, as expected, longer than those pseudo-*trans* to the Cl ligand. If one defines C12L and C34L as the midpoints of the C1L−C2L and C3L−C4L bonds, respectively, then one finds Rh−C12L = 2.157(5) Å and Rh−C34L = 2.002(4) Å. The two C−C(olefin) bond lengths, 1.404(6) and 1.353(6) Å, are significantly different. It would seem that the C3L−C4L bond, 1.404(6) Å, *trans* to the weaker Cl ligand, allows for more selective π-back-bonding and thus a longer C−C bond, whereas the C1L−C2L separation, at 1.353(6) Å, *trans* to the P ligand, is only slightly longer than the ca. 1.34 Å for a routine C−C double bond, and therefore experiences a reduced amount of π-back-bonding.

The figure clearly shows that the four olefinic carbons of the two double bonds are nonequivalent, relative to the positions of the substituents on the P atom, and this is reflected in the NMR spectroscopy. The two double bonds are tilted with respect to the least-squares plane defined by C1L C2L C3L, and C4L, i.e., one is tilted toward the metal and the other in the opposite sense. As found for a number of Rh(1,5-COD)(bidentate)$^+$ cationic complexes,[8,9] the 1,5-COD is slightly rotated relative to the plane defined by the Rh, P, and Cl atoms (see Figure 1).

NMR Studies. Table 2 and Table 3 give ^{13}C, ^{103}Rh, and ^{31}P NMR data for the complexes. While the various ^{31}P chemical shifts are not particularly informative, we note that the values $^1J(^{103}$Rh,^{31}P) for the NBD complexes, ca. 280 Hz, are larger than those for the 1,5-COD analogues, ca. 247 Hz. The ^{1}H spectra of **4**−**8** at 700 MHz are well resolved, and the four nonequivalent olefinic protons can be assigned pairwise via COSY spectroscopy and their respective chemical shifts since those resonances pseudo-*trans* to the P-donor appear at higher frequency. These olefinic ^{1}H signals, in turn, allow the assignment of the olefinic ^{13}C resonances via ^{13}C,^{1}H correlations.

^{13}**C Chemical Shifts.** As expected,[10,11] the olefinic ^{13}C chemical shifts for the carbons pseudo-*trans* to the phosphoramidite P-donor are concentrated at higher frequency, ca.

(4) During the preparation of the manuscript, it was discovered that Mezzetti and co-workers (ETHZ) had also determined the solid-state structure of complex **4**: Mikhel, I. S.; Ruegger, R.; Butti, P.; Camponovo, F.; Huber, D.; Mezzetti, A. *Organometallics* **2008**, *27*, 2937−2948.

(5) (a) Inglesias, M.; Del Pino, C.; Corma, A.; Garcia-Blanco, S.; Carrera, S. M. *Inorg. Chim. Acta* **1987**, *17*, 215–221. (b) Murray, B. D.; Hope, H.; Hvoslef, J.; Power, P. P. *Organometallics* **1984**, *3*, 657–663.

(6) Niyomura, O.; Iwasawa, T.; Sawada, N.; Tokunaga, M.; Obora, Y.; Tsuji, Y. *Organometallics* **2005**, *24*, 3468–3475.
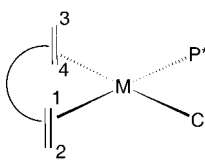
(7) Selent, D.; Baumann, W.; Kempe, R.; Spannenberg, A.; Rottger, D.; Wieser, K. D.; Borner, A. *Organometallics* **2003**, *22*, 4265–4271.

(8) (a) Berger, H.; Nesper, R.; Pregosin, P. S.; Ruegger, H.; Wörle, M. *Helv. Chim. Acta* **1993**, *76*, 1520–1538. (b) Feiken, N.; Pregosin, P. S.; Trabesinger, G. *Organometallics* **1998**, *17*, 4510–4518. (c) Valentini, H.; Selvakumar, K.; Wörle, M.; Pregosin, P. S. *J. Organomet. Chem.* **1999**, *587*, 244–251.

(9) Price, D. W.; Drew, M. G. B.; Hii, K. K.; Brown, J. M. *Chem.−Eur. J.* **2000**, *6*, 4587–4596.

(10) Mann, B. E.; Taylor, B. F. *^{13}C NMR Data for Organometallic Compounds*; Academic Press: London, 1981.

(11) Bonnaire, R.; Davoust, D.; Platzer, N. *Org. Magn. Reson.* **1984**, *22*, 80–85.

Table 2. ^{13}C NMR Chemical Shifts of the Coordinated Double Bonds in the Phosphoramidite Complexes 4−8^{a,b}

	position			
complex	**1**	**2**	**3**	**4**
[RhCl(1,5-COD)]$_2$^{c}	78.6	78.6	78.6	78.6
[RhCl(1,5-COD)(**1**)], **4**	110.8	109.6	74.5	67.9
[RhCl(1,5-COD)(**2**)], **5**	111.8	110.8	74.5	69.1
[RhCl(1,5-COD)(**3**)], **6**	111.7	110.9	73.7	68.9
[RhCl(1,5-COD)(PPh$_3$)]	105.1	105.1	70.8	70.8
[RhCl(NBD)]$_2$^{d}	51.4	51.4	51.4	51.4
[RhCl(NBD)(**1**)], **7**	91.7	89.7	55.3	48.9
[RhCl(NBD)(**2**)], **8**	92.8	91.9	53.2	51.1
[IrCl(1,5-COD)(**2**)], **13**^{d}	102.5	101.7	56.7	52.1
[Rh(1,5-COD)(**1**)$_2$]BF$_4$, **14**	107.8	100.7		
[Rh(1,5-COD)(**3**)$_2$]BF$_4$, **15**	106.5	103.6		

^{a} CD$_2$Cl$_2$, 700 MHz. ^{b} For **4−8**, ^1J(Rh,C) *trans* to P falls in the range 15−20 Hz, with ^2J(P,C) = ca. 6 Hz or less. ^1J(Rh,C) *trans* to Cl falls in the range 11−14 Hz, with ^2J(P,C) not observed. ^{c} 400 MHz. ^{d} From Bonnaire, 263 K.

Table 3. ^{103}Rh^a and ^{31}P NMR Chemical Shifts and ^1J(^{103}Rh,^{31}P)

	δ ^{103}Rh^a	δ ^{31}P	^1J(^{103}Rh)
[RhCl(1,5-COD)(**1**)], **4**	−7882	133.9	247
[RhCl(1,5-COD)(**2**)], **5**	−7979	134.1	247
[RhCl(1,5-COD)(**3**)], **6**	−7963	136.5	247
[RhCl(1,5-COD)(Phosphine)]			
PPh$_3$	−7960,^{b} −7914^a		
PCyPh$_2$,	−7913^b		
PCy$_2$Ph	−7885^b		
[RhCl(1,5-COD)]$_2$	−7242^a		
	−7265^b		
	−7257^b		
[RhCl(NBD))$_2$	−7041^b		
[RhCl(NBD)(**1**)], **7**	−7720	136.9	281
[RhCl(NBD)(**2**)], **8**	−7732	137.7	280
[Rh(1,5-COD)(**1**)$_2$]BF$_4$, **14**	−8385	144.7	246
[Rh(1,5-COD)(**3**)$_2$]BF$_4$, **15**	−8475	145.1	240

^{a} CD$_2$Cl$_2$, 700 MHz, this work. ^{103}Rh chemical shifts are referenced to Rh(acac)$_3$ which lies 8369 ppm (26.447 Hz) to high frequency from 3.16000 MHz as a reference. Benn reports Rh(acac)$_3$ at 3.186447. Benn, R.; Rufinska, A., *Angew. Chem., Int. Ed. Engl.* **1986**, *25*, 861−881. See also: Mann, B. E. Cobalt and Rhodium NMR. In *Transition Metal Nuclear Magnetic Resonance*; Pregosin, P., Ed.; Elsevier: Amsterdam, 1991; pp 143−215. ^{b} (CDCl$_3$ solutions) Bonnaire, R.; Davoust, D.; Platzer, N., *Org. Magn. Reson.* **1984** *22*, 80−85. [RhCl(1,5-COD)]$_2$ has now been measured three times.

110−112 ppm. The values for the olefinic carbons opposite the chloride are spread across a slightly wider range, 7−8 ppm, with one C atom at about 68 ppm and the other at about 74 pm. This relatively larger difference arises presumably due to differing steric effects. The two carbons of this double bond are *cis* to the P-donor and as a consequence experience differing steric interactions with the various fragments of the complexed phosphoramidite (see Figure 1). For the model complexes,[11] RhCl(1,5-COD)(P), P = PPh$_3$, PCyPh$_2$, and PCy$_2$Ph, the ^{13}C values for the olefinic carbons fall in the ranges 102.5−105.1 (*trans* to P) and 70.1−70.7 (*trans* to Cl); see Table 3. Consequently, the olefinic carbons pseudo-*trans* to the P-donors in **4−6** resonate at higher frequency than the models, suggesting somewhat less π-back-bonding from the rhodium. The olefinic ^{13}C chemical shift values for the two NBD complexes **7** and **8** appear ca. 20 ppm to *lower* frequency (relative to the 1,5-COD
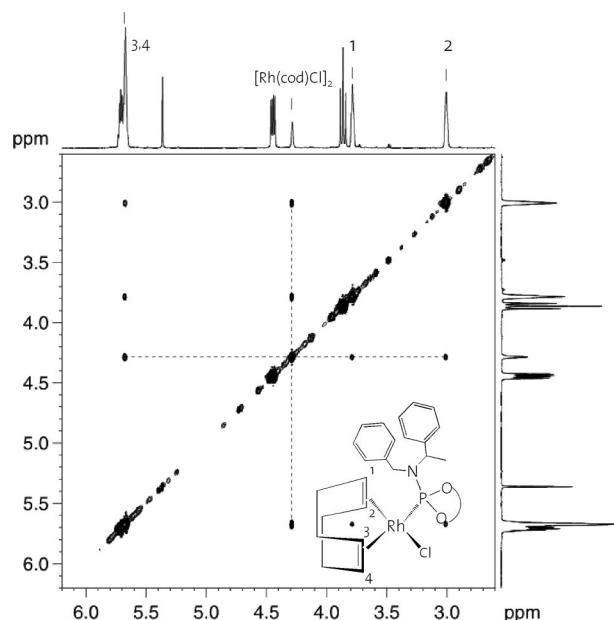

Figure 2. Phase-sensitive NOESY (showing only the exchange cross-peaks) for an isolated sample of **6**, containing ca. 10% of the unreacted dinuclear starting material (whose olefinic signals appear at ca. 4.3 ppm). The exchange cross-peaks with *all four* nonequivalent olefinic resonances of **6** are clearly observed (CD$_2$Cl$_2$, 700 MHz, ambient temperature, mixing time = 800 ms).

complexes), suggesting significantly more π-back-bonding in these derivatives.

Solution Dynamics. 2-D phase-sensitive NOESY measurements were carried out on **4−8**, and Figure 2 shows a section of this spectrum for an isolated sample of **6**, which contains ca.
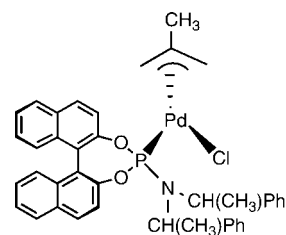
10% of the unreacted dinuclear starting material. Only the exchange cross-peaks, those having the same phase as the diagonal, are shown. The four equivalent olefinic protons for [RhCl(1,5-COD)]$_2$, which appear at ca. 4.3 ppm, can be seen to be exchanging with *all four* nonequivalent olefinic resonances of **6**. This observation is consistent with phosphoramidite dissociation, to afford the starting rhodium dimer, and then recoordination. This type of behavior has been noted previously using 2-D exchange methods,[12] and specifically, we have used this approach (i.e., excess dimer) in our study[12a] of the dynamics of the Pd(allyl)(phosphoramidite) shown above. The analogous NOESY spectrum for the NBD complex **7** (see Figure 3) reveals cross-peaks in keeping with this same type of equilibrium (see the *much weaker* cross-peaks between 2.6 and 4.0 ppm); however, this spectrum is dominated by a set of much stronger cross-peaks from a selective intramolecular exchange process. Although there is some overlap of the two olefinic protons H3 and H4 (pseudo-*trans* to the P-donor), it can be shown that

(12) (a) Filipuzzi, S.; Pregosin, P. S.; Albinati, A.; Rizzato, S. *Organometallics* **2006**, *25*, 5955−5964. (b) Bircher, H.; Bender, B. R.; Von Philipsborn, W. *Magn. Reson. Chem.* **1993**, *31*, 293−298.
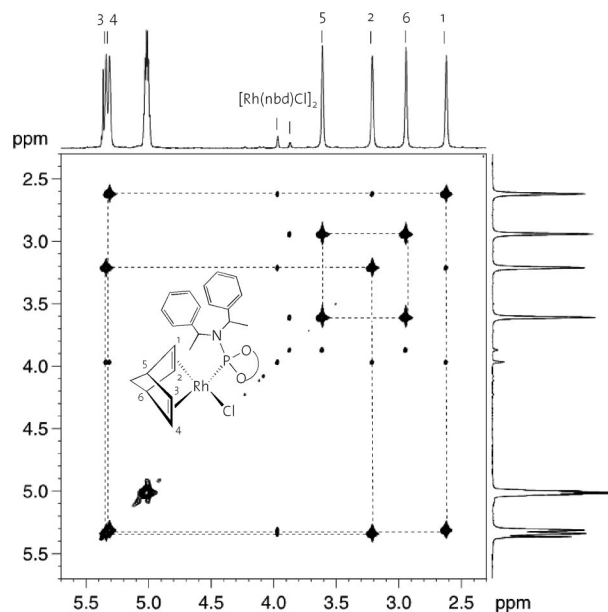
Figure 3. Phase-sensitive NOESY showing only the exchange cross-peaks for an isolated sample of **7** showing a set of relatively strong cross-peaks from a selective intramolecular exchange process involving the olefin protons (CD$_2$Cl$_2$, 700 MHz, ambient temperature, mixing time = 800 ms).

proton H1 exchanges selectively with H4 and that H2 is exchanging with H3. Further, the two aliphatic bridgehead methine protons, H5 and H6, are also exchanging. The 1,5-COD complexes *do not* show this type of exchange. To place these results on a more quantitative scale, and to allow for a very slow exchange in the COD complexes that might go undetected using our NOESY conditions,[13] we have carried out magnetization transfer experiments on the phosphoramidite complexes [RhCl(NBD)(**1**)] and [RhCl(1,5-COD)(**1**)]. We find exchange rates of ca. 5.3 ± 0.2 and ca. 0.1 s^{-1} for these two compounds, respectively; that is, the NBD exchange rate is about 50 times faster than that for the 1,5-COD complex. A series of variable-temperature experiments were then carried out in order to estimate the barrier for the rotation in **7**. On the basis of a line shape analysis of both the olefinic and bridgehead protons, one finds a barrier of ca. 65 kJ/mol. These experimental results for the NBD complexes can be rationalized by postulating diolefin rotation. Several papers have described related isomerization processes involving Rh(diolefin) complexes;[8c,14,15] however, there is no generally accepted mechanism. We will return to this subject in connection with the DFT calculations. Preliminary results suggest that this presumed diolefin rotation is not restricted to phosphoramidite complexes.[16]

Continuing with dynamics, it is known[17] that rotation around the C—C bond connecting the two aryl fragments, for the bipol phosphoramidite **2** (and its Rh complex, **5**), is facile, thereby leading to interconverting diastereomers. This is in contrast to what is found for the naphthyl analogues, **1**, where the energy barriers are much higher. Since we observe only one ^{31}P doublet for **5** at ambient temperature, we have cooled the sample and show the result in Figure 4. At 253 K both diastereomers are clearly visible, although, based on the line shapes, the minor species is clearly still somewhat dynamic on the NMR time scale.

A sample of of [IrCl(1,5-COD)(**2**)], **13**, was prepared in an identical fashion to that for the Rh complex (see Experimental Section). Its ^{31}P NMR spectrum at ambient temperature reveals a broad signal at ca. 114.5 ppm; however at 263 K one observes two signals: a sharp resonance at ca. 114.4 ppm and a weaker, broad resonance at ca. 115.6, in the ratio ca. 12:1, respectively. The ^{1}H,^{1}H 2-D exchange spectra for *both* **5** and **13** at 263 K show that these two presumed diastereomeric species are exchanging slowly on the NMR time scale in both solutions.

^{103}Rh Chemical Shift Data. Although still not a trivial type of NMR measurement, there are an increasing number of reports concerned with ^{103}Rh NMR.[11,18−23] The various ^{103}Rh chemical shifts for **4**−**8** were obtained by 2-D inverse methods (see Figure 5), and these data are found in Table 3, along with chemical shift data for the dinuclear species, [RhCl(1,5-COD)]$_2$ and [RhCl(NBD)]$_2$, plus several related model [RhCl(1,5-COD)-(phosphine)] complexes.

Given the known sensitivity[23] of the metal chemical shift to significant changes in its coordination sphere (hundreds of ppm are not unusual when a new donor is introduced), the data for the 1,5-COD complexes **4**−**8** suggest that the phosphoramidite donor is in no way a special P-donor and rather like a routine tertiary phosphine. Indeed the average of the three chemical shifts for **4**−**6** is −7941, whereas the average of the three values for the model phosphine complexes is −7919. This is a rather modest difference for metal chemical shifts. Although it is clear from the diolefin ^{13}C data that phosphoramidites are different donors than the tertiary phosphines, the rhodium center does not seem to sense this very much. On the other hand, changing from COD to NBD (**4** to **7** or **5** to **8**) affords larger changes in the ^{103}Rh chemical shifts of 162 and 257 ppm, respectively. A similar difference in δ ^{103}Rh, ca. 220 ppm, is found when comparing the metal shifts for the two dinuclear species [RhCl(1,5-COD)]$_2$ and [RhCl(NBD)]$_2$.

(13) At the request of a reviewer, the mixing time in the NOESY experiment for the COD complex **4** was changed. Three new NOESY experiments with mixing times of 600, 900, and 1200 ms were performed. From both the 600 and 900 ms mixing times, there was no evidence for intramolecular olefin exchange; however for the 1200 ms run we do find very weak cross-peaks due to this exchange. This exchange was confirmed by the magnetization transfer experiments.

(14) Crociani, B.; Antonaroli, S.; Di Vona, M. L.; Licoccia, S. *J. Organomet. Chem.* **2001**, *631*, 117–124.

(15) Faller, J. W. In Dynamic NMR Spectroscopy in Organometallic Chemistry. In *Comprehensive Organometallic Chemistry III*; Crabtree R. H., Mingos, D. M. P., Eds.; Elsevier: Oxford, 2006; Vol. 1, pp 407–428.

(16) The 2-D NOESY spectra for the complexes [RhCl(1,5-COD)-(MOP)] and [RhCl(NBD)(MOP)], MOP = 2-diphenylphosphino-1,1′-binaphthyl, reveal the same type of exchange selectivity; that is, we observe di-olefin rotation only in the NBD case.

(17) (a) Mikhel, I. S.; Bernardinelli, G.; Alexakis, A. *Inorg. Chim. Acta* **2006**, *359*, 1826–1836. (b) Alexakis, A.; Polet, D.; Benhaim, C.; Rosset, S. *Tetrahedron: Asymmetry* **2004**, *15*, 2199–2203.

(18) (a) Buhl, M.; Hakansson, M.; Mahmoudkhani, A. H.; Ohrstrom, L. *Organometallics* **2000**, *19*, 5589–5596. (b) von Philipsborn, W. *Chem. Soc. Rev.* **1999**, *28*, 95–105.

(19) (a) Maurer, E.; Rieker, S.; Schollbach, M.; Schwenk, A.; Egolf, T.; von Philipsborn, W. *Helv. Chim. Acta* **1982**, *65*, 26–45. (b) Bender, B. R.; Koller, M.; Nanz, D.; von Philipsborn, W. *J. Am. Chem. Soc.* **1993**, *115*, 5889–5890.

(20) Leitner, W.; Buhl, M.; Fornika, R.; Six, C.; Baumann, W.; Dinjus, E.; Kessler, M.; Kruger, C.; Rufinska, *Organometallics* **1999**, *18*, 1196–1206.

(21) Donkervoort, J. G.; Buhl, M.; Ernsting, J. M.; Elsevier, C. J. *Eur. J. Inorg. Chem.* **1999**, 27–33. (a) Aizenberg, M.; Ott, J.; Elsevier, C. J.; Milstein, D. *J. Organomet. Chem.* **1998**, *551*, 81–92.

(22) (a) Donkervoort, J. G.; Buhl, M.; Ernsting, J. M.; Elsevier, C. J. *Eur. J. Inorg. Chem.* **1999**, *2*, 7–33. (b) Aizenberg, M.; Ott, J.; Elsevier, C. J.; Milstein, D. *J. Organomet. Chem.* **1998**, *551*, 81–92. (c) Heaton, B. T.; Iggo, J. A.; Podkorytov, I. S.; Smawfield, D. J.; Tunik, S. P.; Whyman, R. *J. Chem. Soc., Dalton Trans.* **1999**, 1917–1919.

(23) Pregosin, P. S. *Inorganic Nuclei: Low Sensitivity Transition Metals*; John Wiley & Sons Ltd.: Chichester, 1996; Vol. 4, pp 2549−2557.
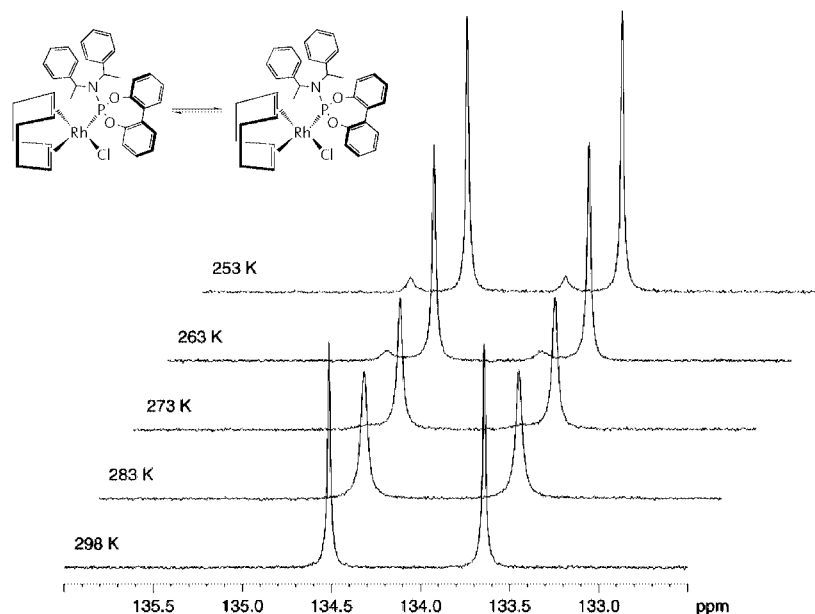
Figure 4. Variable-temperature ^{31}P spectra for **5**. The two interconverting diastereomers can be seen at 253 K (CD$_2$Cl$_2$, 700 MHz, ambient temperature).
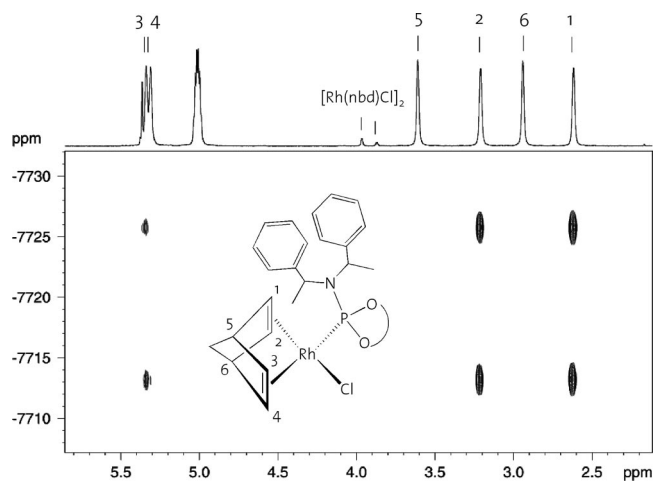

Figure 5. 2-D ^{103}Rh,^{1}H spectrum for **7** (CD$_2$Cl$_2$, 700 MHz, ambient temperature).

Bis-phosphoramidite Complexes. Addition of 2 equiv of phosphoramidites **1** and **3** to [Rh(1,5-COD)]$_2$(BF$_4$) affords the bis complexes [Rh(1,5-COD)(**1**)$_2$]BF$_4$, **14**, and [Rh(1,5-COD)(**3**)$_2$]BF$_4$, **15**, respectively. These could be satisfactorily characterized via microanalytical data together with ^{103}Rh, ^{31}P, and ^{13}C NMR measurements (e.g., for **14**, δ ^{31}P = 144.7, $^{1}J(^{103}$Rh,^{31}P) = 246 Hz). The ^{103}Rh spectra reveal the expected triplet structure due to the presence of two ^{31}P spins, and the metal chemical shifts for both complexes appear in Table 3. It is interesting that one can readily complex two such large P-donors in *cis* position. A related *cis* geometry has already been reported for a Pd(II) complex.[13] We note that Selent et al.,[7] in their hydroformylation chemistry, and Reetz and co-workers,[3c] in their hydrogenation studies, suggest that two very bulky phosphite donors can complex to rhodium; however, these structures are not proven unambiguously.

DFT Calculations. To understand the differing dynamic processes associated with the diolefin ligands in the RhCl(diolefin)-(phosphoramidite) complexes, we have carried out a number of DFT calculations.[24] Given the size of phosphoramidite **1**, a model of this ligand was used in the calculations. In this model, **1′**, the binaphthyl groups attached to the O atoms have been replaced by a biphenyl moiety, and the α-phenethyl substituents on the nitrogen by isopropyl groups.

1′
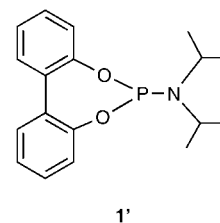
Comparison of the structure optimized for the model complex containing 1,5-COD, **4′**, with the experimental structure determined for **4** provides a test for the performance of the computational method employed. The overall geometry is the same in both **4** and **4′** and corresponds to a pseudo-square-planar arrangement around the rhodium atom with the P and chloride ligands occupying two adjacent coordination positions and the 1,5-COD double bonds occupying the remaining two positions. The square-planar environment of **4′** is reflected in a 5° angle between the RhPCl plane and the plane defined by Rh and the centers of the C=C bonds. The Rh−(donor) coordination distances are also well reproduced in the calculated structure, with maximum and mean absolute deviations of 0.054 and 0.023 Å, respectively, when compared to the X-ray structure. In addition, the calculated P−Rh−Cl and c$_1$−Rh−c$_2$ angles (c$_1$ and c$_2$ being the center of the C=C bonds) are within 1° of the experimental structures. These results demonstrate that the DFT method employed provides a good description of the system studied, at least from the structural point of view, and validates the choice of the simplified model phosphoramidite ligand, **1′**. For example, it is interesting to note that the differing *trans* influences of the phosphoramidite and chloride ligands, observed in the X-ray structure of **4**, are well reproduced in the calculated

(24) Parr, R. G.; Yang, W. *Density Functional Theory of Atoms and Molecules*; Oxford University Press: New York, 1989.
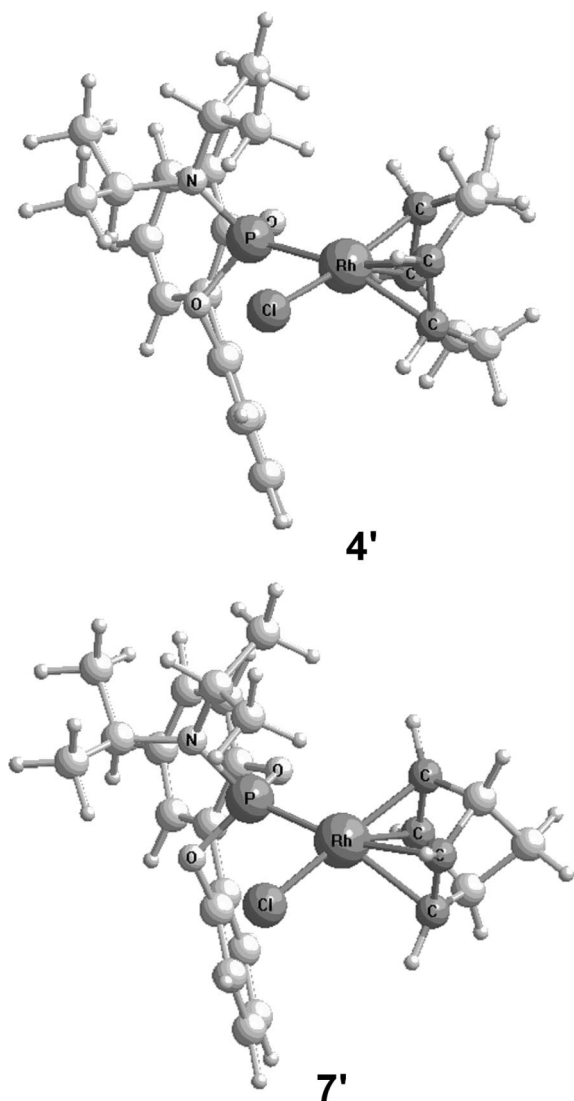
charge, obtained by means of a natural population analysis (NPA),[26] is 0.10 in both complexes.

The mechanism for rotation of the diolefin ligand in both **4′** and **7′** was investigated in order to try to understand the fluxional behavior observed for the NBD in **7**, but absent in the analogous 1,5-COD complexes. The calculated mechanism corresponds, in both cases, to a single-step path with the geometry around the metal changing from pseudo-square-planar in the minima (**4′** and **7′**) to pseudotetrahedral in the transition states, **TS$_{4'}$** and **TS$_{7'}$** (see Figure 7). The pseudotetrahedral geometry of the transition states is shown by the angle between the RhPCl plane and the plane defined by the metal and the two C=C centers: 83° for **TS$_{4'}$** and 81° for **TS$_{7'}$**. These values approach the angle expected for a perfect tetrahedral coordination (90°). During the rotation, the two diolefin C=C bonds remain coordinated to the metal. In fact, in the transition states, **TS$_{4'}$** and **TS$_{7'}$**, four equivalent Rh−C distances of about 2.1 Å are observed. This is clearly different from the ground-state structures, where two sets of Rh−C distances exist due to differing *trans* influences of the phosphoramidite and chloride ligands (around 2.2 Å for the C=C opposite the P atom and ca. 2.1 Å for the C=C bond *cis* to the Cl atom). The *cis/trans* orientations existing in the square-planar geometry of the ground state are no longer present in the tetrahedral arrangement of the transition states, and thus, the distortion due to the phosphoramidite *trans* influence is also lost.

The structures calculated for the two transition states **TS$_{4'}$** and **TS$_{7'}$** are completely equivalent with respect to the Rh−C and the Rh−Cl bonds, with distances within 0.01 Å and Wiberg indices within 0.02, when comparing the corresponding bonds in the two species. The major difference between **TS$_{4'}$** and **TS$_{7'}$** involves the Rh−P bond (Figure 7). In the NBD case, that is in **TS$_{7'}$**, the Rh−P bond is significantly shorter (2.400 Å) and stronger (WI = 0.312) than the corresponding bond in the 1,5-COD case, **TS$_{4'}$** (d_{Rh-P} = 2.470 Å, WI = 0.261). Presumably, the calculated difference between the Rh−P bonds arises from steric effects. The tetrahedral arrangement in the transition states brings the coordinated C=C double bonds of the diolefin in close proximity to the bulky substituents on the phosphoramidite ligand. One C=C bond approaches the biphenyl substituent of the O atom, whereas the other C=C bond is close to the N atom substituents. The larger bite angle[27] of 1,5-COD (87°, relative to that for NBD, 70°) means that the two 1,5-COD double bonds are further apart in **TS$_{4'}$** and, thus, closer to the phosphoramidite substituents. Hence, there is increased interligand repulsion between diene and phosphoramidite in **TS$_{4'}$**, when compared to **TS$_{7'}$**, pushing the phosphoramidite ligand away and resulting in a longer and weaker Rh−P bond in **TS$_{4'}$**.

A weaker Rh−P bond in **TS$_{4'}$** corresponds to a weaker electron donation from the phosphoramidite ligand to the metal. As a consequence, the Rh atom is more positive in **TS$_{4'}$** than in **TS$_{7'}$**, the corresponding NPA charges being 0.38 and 0.32, respectively. An electron poorer rhodium atom in **TS$_{4'}$** leads to

Figure 6. Optimized geometry for the [RhCl(diene)(**1′**)] complexes with diene = 1,5-COD (**4′**, top) and NBD (**7′**, bottom). The metal and the coordinated atoms are dark gray.

geometry of **4′** with the Rh−C bond lengths longer by ca. 0.1 Å for the C=C bond opposite the P atom.

The geometry calculated for the NBD model complex, **7′**, also shown in Figure 6, is completely equivalent to the one presented by **4′**. The pseudo-square-planar coordination geometry is once again indicated by an angle of 1° between the RhPCl plane and the plane defined by the metal and the centers of the C=C double bonds (c_1−Rh−c_2). In addition, the deviation between the Rh−(donor) coordination distances in **7′** and the corresponding separations in **4′** is <0.03 Å. In **7′**, as in **4′**, the Rh−C distances associated with the C=C bond *trans* to the phosphoramidite ligand are about 0.1 Å longer than the corresponding separations *trans* to the chloride. The similarity between the two complexes **4′** and **7′** is not only geometric. Thus, a comparison of the Wiberg indices[25] calculated for all Rh−(donor) bonds reveals that these are within 0.01, for the corresponding bonds in the two molecules. In addition, the metal

(25) (a) Wiberg, K. B. *Tetrahedron* **1968**, *24*, 1083. (b) Wiberg indices are electronic parameters related to the electron density between atoms. They can be obtained from a natural population analysis and provide an indication of the bond strength.

(26) (a) Carpenter, J. E.; Weinhold, F. *J. Mol. Struct. (THEOCHEM)* **1988**, *169*, 41. (b) Carpenter, J. E. Ph.D. Thesis, University of Wisconsin, Madison WI, 1987. (c) Foster, J. P.; Weinhold, F. *J. Am. Chem. Soc.* **1980**, *102*, 7211. (d) Reed, A. E.; Weinhold, F. *J. Chem. Phys.* **1983**, *78*, 4066. (e) Reed, A. E.; Weinhold, F. *J. Chem. Phys.* **1983**, *78*, 1736. (f) Reed, A. E.; Weinstock, R. B.; Weinhold, F. *J. Chem. Phys.* **1985**, *83*, 735. (g) Reed, A. E.; Curtiss, L. A.; Weinhold, F. *Chem. Rev.* **1988**, *88*, 899. (h) Weinhold, F.; Carpenter, J. E. *The Structure of Small Molecules and Ions*; Plenum: New York, 1988; p 227.
(27) The bite angle is defined as the angle c_1−Rh−c_2, c_1 and c_2 being the centers of the C=C bonds. The bite angle calculated for 1,5-COD is 87° in both species **4′** and **TS$_{4'}$**; the bite angle calculated for NBD is 71° in **7′** and 70° in **TS$_{7'}$**.
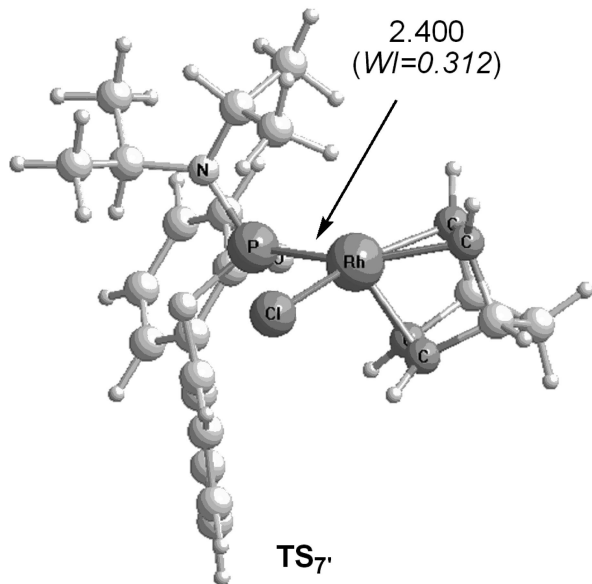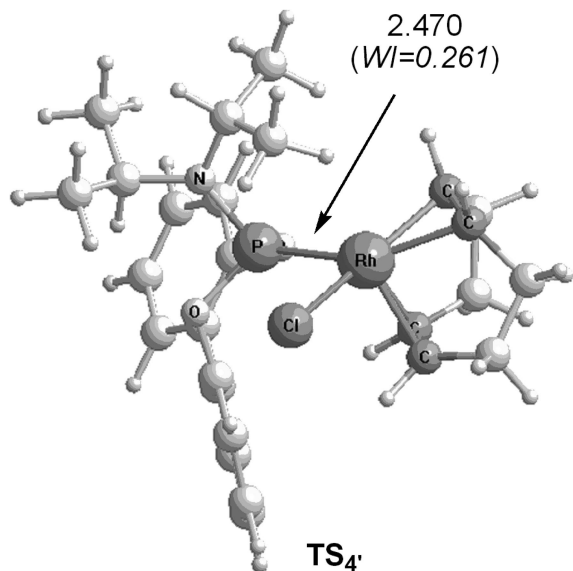
Figure 7. Optimized geometry for the transition state of 1,5-COD rotation in **4′** (**TS₄′**, top) and NBD rotation in **7′** (**TS₇′**, bottom). The Rh−P distance and the corresponding Wiberg index (WI, italics) are indicated. The metal and the coordinated atoms are dark gray.

a less stable species, relative to **TS₇′**, and, thus, to a higher energy barrier for diene rotation, in good agreement with the

(28) Frisch, M. J.; Trucks, G. W.; Schlegel, H. B.; Scuseria, G. E.; Robb, M. A.; Cheeseman, J. R.; Montgomery, J. A., Jr.; Vreven, T.; Kudin, K. N.; Burant, J. C.; Millam, J. M.; Iyengar, S. S.; Tomasi, J.; Barone, V.; Mennucci, B.; Cossi, M.; Scalmani, G.; Rega, N.; Petersson, G. A.; Nakatsuji, H.; Hada, M.; Ehara, M.; Toyota, K.; Fukuda, R.; Hasegawa, J.; Ishida, M.; Nakajima, T.; Honda, Y.; Kitao, O.; Nakai, H.; Klene, M.; Li, X.; Knox, J. E.; Hratchian, H. P.; Cross, J. B.; Adamo, C.; Jaramillo, J.; Gomperts, R.; Stratmann, R. E.; Yazyev, O.; Austin, A. J.; Cammi, R.; Pomelli, C.; Ochterski, J. W.; Ayala, P. Y.; Morokuma, K.; Voth, G. A.; Salvador, P.; Dannenberg, J. J.; Zakrzewski,V. G.; Dapprich, S.; Daniels, A. D.; Strain, M. C.; Farkas, O.; Malick, D. K.; Rabuck, A. D.; Raghavachari, K.; Foresman, J. B.; Ortiz, J. V.; Cui, Q.; Baboul, A. G.; Clifford, S.; Cioslowski, J.; Stefanov, B. B.; Liu, G.; Liashenko, A.; Piskorz, P.; Komaromi, I.; Martin, R. L.; Fox, D. J.; Keith, T.; Al-Laham, M. A.; Peng, C. Y.; Nanayakkara, A.; Challacombe, M.; Gill, P. M. W.; Johnson, B.; Chen,W.; Wong, M. W.; Gonzalez, C.; Pople, J. A. *Gaussian 03, Revision C.02*; Gaussian, Inc.: Wallingford, CT, 2004.
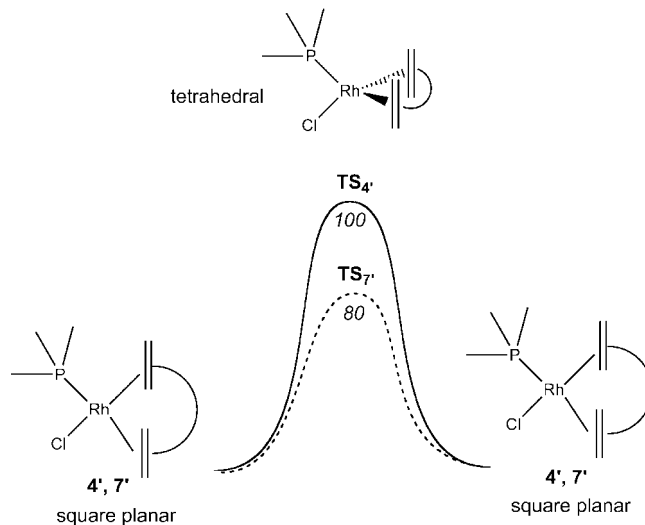

Figure 8. Energy barriers (kJ/mol, italics) for the rotation of 1,5-COD in **4′** (solid line) and of NBD in **7′** (dashed line).

experimental NMR studies. The energy profiles obtained for the two model complexes are represented in Figure 8.

The calculated activation energy for NBD rotation in **7′**, 80 kJ/mol (19 kcal/mol), is only in fair agreement with the experimental result and reflects the limitations of the simplified model used in the calculations.

Conclusions

The various physical studies on these RhCl(diene)(phosphoramidite-type) complexes suggest that both electronic and steric effects affect the nature of the olefin, chloride, and P-donor bonding. The X-ray study reveals an interesting intramolecular selectivity in the back-bonding. Two types of dynamic processes have been detected at ambient temperature in CD_2Cl_2 solution: (a) exchange with [RhCl(diene)]₂, via presumed (but not proven) phosphoramidite dissociation, and (b) diolefin rotation. The former is readily observed with both the 1,5-COD and NBD complexes. The latter is more selective in that the intramolecular dynamics for the NBD analogues are relatively fast, but those for the 1,5-COD compounds, barely detectable. The interconversion of the diastereomeric complexes from the binol ligand **2** is slow on the NMR time scale at around 253 K. DFT calculations suggest that the diolefin rotation proceeds over a tetrahedral transition state, *without* Rh−olefin bond breaking, and that there is a smaller energy barrier for the NBD complexes relative to the analogous 1,5-COD species, presumably for steric reasons.

Experimental Part

General Procedures. All reactions and manipulations were performed under a N₂ atmosphere using standard Schlenk techniques. The rhodium precursors [Rh(1,5-COD)Cl]₂ and [Rh(NBD)Cl]₂ (1,5-COD = 1,5-cyclooctadiene, NBD = [2.2.1]hepta-2,5-diene, norbornadiene) were purchased from commercial sources and used as received from the producer. Solvents were dried and distilled under standard procedures and stored under nitrogen. NMR spectra were recorded with Bruker DPX-250, 300, 400, 500, and 700 MHz spectrometers at room temperature, unless otherwise stated. Further details with respect to the NMR data are presented in the Supporting Information. Chemical shifts are given in ppm; coupling constants (*J*) in hertz. Elemental analyses and mass spectroscopic studies were performed at the ETHZ.

Line Shape Analysis. A series of ^{1}H spectra for complex **7** in $C_2D_2Cl_4$ at different temperatures (from 300 to 340 K, at intervals of 5 K) were recorded on a Bruker Advance spectrometer, 700 MHz. The sample temperature was controlled by a Bruker BVT 3000 digital unit. After a phase and baseline correction, the half-height line widths ($\Delta_{1/2}$) of the olefinic and bridgehead protons of norbornadiene were measured.

$$k = (\Delta_{1/2} - \Delta_{\text{ref}})\pi = A_0 e^{(-E_a/RT)}$$

Using the relation where Δ_{ref} is the line width of the signal, which was estimated to be equal to 12.6 Hz, a plot of $\ln(k)$ against $1/T$ gives a value for the activation energy E_a. The 12.6 Hz estimate derives from the fact that the olefinic protons are part of a modestly complicated spin system.

Computational Details. All calculations reported in the text were performed using the Gaussian 03 software package[28] and the PBE1PBE functional, without symmetry constraints. That functional uses a hybrid generalized gradient approximation (GGA), including 25% mixture of Hartree−Fock[29] exchange with DFT[24] exchange−correlation, given by the Perdew, Burke, and Ernzerhof functional (PBE).[30] The optimized geometries were obtained with the LanL2DZ basis set[31] augmented with an f-polarization function[32] for Mo, the same basis set augmented with a d-polarization function[33] for P and Cl, and a standard 6-31G(d,p)[34] for the remaining elements (basis b1). Transition-state optimizations were performed with the synchronous transit-guided quasi-Newton method (STQN) developed by Schlegel et al.[35] Frequency calculations were performed to confirm the nature of the stationary points, yielding one imaginary frequency for the transition states and none for the minima. Each transition state was further confirmed by following its vibrational mode downhill on both sides and obtaining the minima presented on the energy profiles. A natural population analysis (NPA)[26] and the resulting Wiberg indices[25] were used to study the electronic structure and bonding of the optimized species.

Energy barriers reported in Figure 8 result from single-point energy calculations using a VTZP basis set (basis b2), and the geometries were optimized at the PBE1PBE/b1 level. Basis b2 consisted of Stuttgart/Dresden ECP with valence triple-ζ (SDD)[36] and an added f-polarization function[32] for Mo, and standard

6-311++G(d,p)[37] for the remaining elements. Solvent (dichloromethane) effects were considered in the PBE1PBE/b2//PBE1PBE/b1 energy calculations using the polarizable continuum model (PCM) initially devised by Tomasi and co-workers[38] as implemented in Gaussian 03,[39] and thus, the energy barriers in Figure 8 can be taken as free energy.[40] The molecular cavity was based on the united atom topological model applied on UAHF radii, optimized for the HF/6-31G(d) level.

The tetrahedral high-spin isomers ($S = 1$) were optimized for both **4′** and **7′**, being, in both cases, less stable than the corresponding transition states, **TS$_{4'}$** and **TS$_{7'}$**. At the PBE1PBE/b1 level, the tetrahedral complex with 1,5-COD (^{1}**4′**) is 20.5 kJ/mol less stable than **TS$_{4'}$**, and the high-spin tetrahedral complex of NBD (^{1}**7′**) is 39.3 kJ/mol less stable than **TS$_{7'}$**.

[Rh(1,5-COD)$_2$]BF$_4$.[41a] and the phosphoramidite ligands (S,S,S)-**1**, (S,S)-**2**, and (S,S)-**3** were synthesized according to published procedures.[41b,c]

Synthesis of [RhCl(diene)(phosphoramidite)]. A solution of the P-donor ligand (0.180 mmol, 2.0 equiv) in CH$_2$Cl$_2$ (7 mL) is slowly added, under stirring, to a solution of the suitable dinuclear species [Rh(diene)Cl]$_2$ (0.090 mmol, 1.0 equiv) in CH$_2$Cl$_2$ (7 mL). After the addition is finished, the solution is stirred for 15 min, and then the solvent removed under reduced pressure. The crude solid, which results, is washed with diethyl ether and dried under vacuum.

[RhCl(1,5-COD)(1)] (4): bright yellow solid, yield 83%. Anal. Calcd for C$_{44}$H$_{44}$ClNO$_2$PRh: C, 67.05; H, 5.63; N, 1.78. Found: C, 66.51; H, 5.54; N, 1.83. MALDI MS: 750 (M$^+$ − Cl), 642 (M$^+$ − Cl − COD), 540 (M$^+$ − Cl − COD − Rh). Crystals suitable for X-ray diffraction were obtained by layering diethyl ether over a saturated solution of the complex in CH$_2$Cl$_2$.

[RhCl(1,5-COD)(2)] (5): light orange, yield 92%. Anal. Calcd for C$_{36}$H$_{38}$ClNO$_2$PRh·H$_2$O: C, 61.42; H, 5.72; N, 1.99. Found: C, 61.26; H, 5.30; N, 1.96. MALDI MS: 650 (M$^+$ − Cl), 542 (M$^+$ − Cl − COD), 440 (M$^+$ − Cl − COD − Rh).

[RhCl(1,5-COD)Cl(3)] (6): yellow solid, yield 88%. Anal. Calcd for C$_{43}$H$_{40}$ClNO$_2$PRh·H$_2$O: C, 65.37; H, 5.36; N, 1.77. Found: C, 65.75; H, 5.51; N, 1.70. MALDI MS: 1153 (M$^+$ − Cl − COD + **2**), 736 (M$^+$ − Cl), 628 (M$^+$ − Cl − COD), 526 (M$^+$ − Cl − COD − Rh).

[RhCl(NBD)(1)] (7): yellow-orange solid, yield 87%. Anal. Calcd for C$_{43}$H$_{38}$ClNO$_2$PRh·H$_2$O: C, 65.53; H, 5.12; N, 1.78. Found: C, 65.57; H, 4.91; N, 1.75. MALDI MS: 734 (M$^+$ − Cl), 642 (M$^+$ − Cl − NBD), 540 (M$^+$ − Cl − NBD − Rh).

[RhCl(NBD)(2)] (8): orange solid, yield 91%. Anal. Calcd for C$_{35}$H$_{33}$ClNO$_2$PRh: C, 62.84; H, 4.97; N, 2.09. Found: C, 62.40; H, 5.34; N, 2.09. MALDI MS: 981 (M$^+$ − Cl − NBD + **1**), 634 (M$^+$ − Cl), 440 (M$^+$ − Cl − NBD − Rh).

Synthesis of [IrCl(1,5-COD)(2)], 13. A solution of the P-donor ligand (0.180 mmol, 2.0 equiv) in CH$_2$Cl$_2$ (7 mL) is slowly added, under stirring, to a solution of the dinuclear species [Ir(1,5-

(29) Hehre, W. J.; Radom, L.; Schleyer, P. v. R.; Pople, J. A. *Ab Initio Molecular Orbital Theory*; John Wiley & Sons: New York, 1986.

(30) (a) Perdew, J. P.; Burke, K.; Ernzerhof, M. *Phys. Rev. Lett.* **1997**, *78*, 1396. (b) Perdew, J. P. *Phys. Rev. B* **1986**, *33*, 8822.

(31) (a) Dunning, T. H., Jr.; Hay, P. J. In *Modern Theoretical Chemistry*; Schaefer, H. F., III, Ed.;Plenum: New York,1976; Vol. 3, p 1. (b) Hay, P. J.; Wadt, W. R. *J. Chem. Phys.* **1985**, *82*, 270. (c) Wadt, W. R.; Hay, P. J. *J. Chem. Phys.* **1985**, *82*, 284. (d) Hay, P. J.; Wadt, W. R. *J. Chem. Phys.* **1985**, *82*, 2299.

(32) Ehlers, A. W.; Böhme, M.; Dapprich, S.; Gobbi, A.; Höllwarth, A.; Jonas, V.; Köhler, K. F.; Stegmann, R.; Veldkamp, A.; Frenking, G. *Chem. Phys. Lett.* **1993**, *208*, 111.

(33) Höllwarth, A.; Böhme, M.; Dapprich, S.; Ehlers, A. W.; Gobbi, A.; Jonas, V.; Köhler, K. F.; Stegmann, R.; Veldkamp, A.; Frenking, G. *Chem. Phys. Lett.* **1993**, *208*, 237.

(34) (a) Ditchfield, R.; Hehre, W. J.; Pople, J. A. *J. Chem. Phys.* **1971**, *54*, 724. (b) Hehre, W. J.; Ditchfield, R.; Pople, J. A. *J. Chem. Phys.* **1972**, *56*, 2257. (c) Hariharan, P. C.; Pople, J. A. *Mol. Phys.* **1974**, *27*, 209. (d) Gordon, M. S. *Chem. Phys. Lett.* **1980**, *76*, 163. (e) Hariharan, P. C.; Pople, J. A. *Theor. Chim. Acta* **1973**, *28*, 213.

(35) (a) Peng, C.; Ayala, P. Y.; Schlegel, H. B.; Frisch, M. J. *J. Comput. Chem.* **1996**, *17*, 49. (b) Peng, C.; Schlegel, H. B. *Isr. J. Chem.* **1994**, *33*, 449.

(36) (a) Häussermann, U.; Dolg, M.; Stoll, H.; Preuss, H.; Schwerdtfeger, P.; Pitzer, R. M. *Mol. Phys.* **1993**, *78*, 1211. (b) Kuechle, W.; Dolg, M.; Stoll, H.; Preuss, H. *J. Chem. Phys.* **1994**, *100*, 7535. (c) Leininger, T.; Nicklass, A.; Stoll, H.; Dolg, M.; Schwerdtfeger, P. *J. Chem. Phys.* **1996**, *105*, 1052.

(37) (a) McClean, A. D.; Chandler, G. S. *J. Chem. Phys.* **1980**, *72*, 5639. (b) Krishnan, R.; Binkley, J. S.; Seeger, R.; Pople, J. A. *J. Chem. Phys.* **1980**, *72*, 650. (c) Wachters, A. J. H. *J. Chem. Phys.* **1970**, *52*, 1033. (d) Hay, P. J. *J. Chem. Phys.* **1977**, *66*, 4377. (e) Raghavachari, K.; Trucks, G. W. *J. Chem. Phys.* **1989**, *91*, 1062. (f) Binning, R. C.; Curtiss, L. A. *J. Comput. Chem.* **1995**, *103*, 6104. (g) McGrath, M. P.; Radom, L. *J. Chem. Phys.* **1991**, *94*, 511.

(38) (a) Cancès, M. T.; Mennucci, B.; Tomasi, J. *J. Chem. Phys.* **1997**, *107*, 3032. (b) Cossi, M.; Barone, V.; Mennucci, B.; Tomasi, J. *Chem. Phys. Lett.* **1998**, *286*, 253. (c) Mennucci, B.; Tomasi, J. *J. Chem. Phys.* **1997**, *106*, 5151.

(39) Tomasi, J.; Mennucci, B.; Cammi, R. *Chem. Rev.* **2005**, *105*, 2999.

(40) Cossi, M.; Scalmani, G.; Rega, N.; Barone, V. *J. Chem. Phys.* **2002**, *117*, 43.

(41) (a) Chatt, J.; Venanzi, L. M. *J. Chem. Soc.* **1957**, *473*, 5–4741. (b) Arnold, L. A.; Imbos, R.; Mandoli, A.; de Vries, A. H. M.; Naasz, R.; Feringa, B. L. *Tetrahedron* **2000**, *56*, 2865–2878. (c) Alexakis, A.; Rosset, S.; Allamand, J.; March, S.; Guillen, F.; Benhaim, C. *Synlett* **2001**, *9*, 1375–1378.

COD)Cl]$_2$ (0.090 mmol, 1.0 equiv) in CH$_2$Cl$_2$ (7 mL). After the addition is finished, the solution is stirred for 15 min, then the solvent is removed under reduced pressure, giving a solid, which is washed with diethyl ether and dried under vacuum to afford [IrCl(1,5-COD)(**2**)], as a red-orange solid in 87% yield. See supplementary tables for NMR details. Anal. Calcd for C$_{36}$H$_{38}$ClNO$_2$PIr: C, 55.75; H, 4.94; N, 1.81. Found: C, 55.92; H, 5.11; N, 1.73. MALDI MS *m/e* = 738 (M − Cl$^+$).

Synthesis of [Rh(diene)(phosphoramidite)$_2$]BF$_4$. A solution of the P-donor ligand (0.280 mmol, 2.0 equiv) in CH$_2$Cl$_2$ (7 mL) is slowly added, under stirring, to a solution of [Rh(1,5-COD)$_2$]BF$_4$ (0.140 mmol, 1.0 equiv) in CH$_2$Cl$_2$ (7 mL). After the addition is finished, the solution is stirred for 15 min, then it is concentrated under reduced pressure to a volume of about 0.5 mL. The product precipitates as a yellow-orange solid. The crude product is filtered, washed with diethyl ether, and then dried under vacuum.

[Rh(1,5-COD)(1)$_2$]BF$_4$, 14: orange solid, yield 78%. Anal. Calcd for C$_{80}$H$_{72}$N$_2$O$_4$BF$_4$P$_2$Rh · H$_2$O: C, 68.87; H, 5.35; N, 2.01. Found: C, 68.67; H, 5.37; N, 1.91. MALDI MS: 1181 (M$^+$ − BF$_4$ − COD), 642 (M$^+$ − BF$_4$ − COD − **1**).

[Rh(1,5-COD)(3)$_2$]BF$_4$, 15: orange solid, yield 75%. Anal. Calcd for C$_{78}$H$_{68}$N$_2$O$_4$BF$_4$P$_2$Rh: C, 69.45; H, 5.08; N, 2.08. Found: C, 68.87; H, 5.28; N, 1.98.

Crystallography. Air-stable, yellow crystals of [RhCl(1,5-COD)(**1**)])]·CH$_2$Cl$_2$, (**4**)·CH$_2$Cl$_2$, suitable for X-ray diffraction were obtained by layering diethyl ether over a saturated solution of the complex in CH$_2$Cl$_2$. A crystal of **4**·CH$_2$Cl$_2$ was mounted on a Bruker APEX II diffractometer, equipped with a CCD detector, and cooled, using a cold nitrogen stream, to 120(2) K for the data collection.

The space group was determined from the systematic absences, while the cell constants were refined at the end of the data collection with the data reduction software SAINT.[42] The experimental conditions for the data collections and crystallographic and other relevant data are listed in Table 4 and in the Supporting Information.

The collected intensities were corrected for Lorentz and polarization factors[42] and empirically for absorption using the SADABS program.[43] The structure was solved by direct and Fourier methods and refined by full matrix least-squares,[44] minimizing the function $[\sum w(F_o^2 - (1/k)F_c^2)^2]$. From the Fourier difference maps a clathrated CH$_2$Cl$_2$ molecule was also found. All atoms, except the hydrogens, were refined using anisotropic displacement parameters. No extinction correction was deemed necessary. Upon convergence, the final Fourier difference map showed no significant features.

The contribution of the hydrogen atoms, in their calculated positions, was included in the refinement using a riding model (B(H) = aB(C$_{bonded}$)(Å^2), where a = 1.5 for the hydrogen atoms of the

Table 4. Experimental Data for the X-ray Diffraction Study of Compound [RhCl(1,5-COD)(1)]·CH$_2$Cl$_2$, (4)·CH$_2$Cl$_2$

formula	C$_{45}$H$_{44}$Cl$_3$NO$_2$PRh
mol wt	871.04
data coll *T*, K	120(2)
diffractometer	Bruker APEX II CCD
cryst syst	monoclinic
space group (no.)	*P*2$_1$(4)
a, Å	11.234(2)
b, Å	11.493(3)
c, Å	15.839(1)
θ, deg	103.231(4)
V, Å^3	1990.7(6)
Z	2
$\rho_{(calcd)}$, g cm^{-3}	1.453
μ, cm^{-1}	7.10
radiation	Mo Kα (graphite monochrom, λ = 0.71073 Å)
θ range, deg	1.86 < θ < 26.03
no. data collected	18 258
no. indep data	7806
no. obsd reflns (n_o) [$|F_o|^2 > 2.0\sigma(|F|^2)$]	7322
no. of params refined (n_v)	478
absolute struct param	−0.04(2)
R_{int}^{a}	0.0317
R(obsd reflns)^b	0.0355
R^2_w(obsd reflns)^c	0.0875
GOF^d	1.046

^{a} $R_{int} = \sum|F_o^2 - \langle F_o^2 \rangle|/\sum F_o^2$. ^{b} $R = \sum(|F_o - (1/k)F_c|)/\sum|F_o|$. ^{c} $R_w^2 = \{\sum[w(F_o^2 - (1/k)F_c^2)^2]/\sum w|F_o^2|^2]\}^{1/2}$. ^{d} GOF = $[\sum_w(F_o^2 - (1/k)F_c^2)^2/(n_o - n_v)]^{1/2}$.

methyl groups and a = 1.2 for the others). Refining the Flack's parameter tested the handedness of the structure.[46]

The scattering factors used, corrected for the real and imaginary parts of the anomalous dispersion, were taken from the literature.[45] All calculations were carried out by using the PC version of the programs WINGX,[47] SHELX-97,[44] and ORTEP.[48]

Supporting Information Available: Full numbering system for **4**, plus cif files. This material is available free of charge via the Internet at http://pubs.acs.org.

OM800082C

(42) BrukerAXS. *SAINT Integration Software*; Bruker Analytical X-ray Systems: Madison, WI, 1995.
(43) Sheldrick, G. M. *SADABS, Program for Absorption Correction*; Universität Göttingen, 1996.
(44) Sheldrick, G. M. *SHELX-97, Structure Solution and Refinement Package*; Universität Göttingen, 1997.

(45) *International Tables for X-ray Crystallography*; Wilson, A. J. C., Ed.; Kluwer Academic Publisher: Dordrecht, The Netherlands,1992; Vol. C.
(46) Flack, H. D. *Acta Crystallogr.* **1983**, *A39*, 876.
(47) Farrugia, L. J. *J. Appl. Crystallogr.* **1999**, *32*, 837.
(48) Farrugia, L.J. *J. Appl. Crystallogr.* **1997**, *30*, 565.